Allylic Oxidation of Cyclohexene and Indene by *cis*-$[Ru^{IV}(bpy)_2(py)(O)]^{2+}$

Laura K. Stultz,[†] My Hang V. Huynh,[||] Robert A. Binstead,[‡] Maria Curry, and Thomas J. Meyer*[,§]

Contribution from the Department of Chemistry, Venable and Kenan Laboratories, The University of North Carolina at Chapel Hill,Chapel Hill, North Carolina 27599-3290

Received May 24, 1999

Abstract: The kinetics of oxidation of cyclohexene, cyclohexen-1-ol, and indene by *cis*-$[Ru^{IV}(bpy)_2(py)(O)]^{2+}$ (bpy = 2,2′-bipyridine and py = pyridine) have been studied in CH_3CN. The reactions are first-order in both $Ru^{IV}{=}O^{2+}$ and substrate in an initial, rapid stage in which Ru(IV) is reduced to Ru(III). The rate constants are 0.16 ± 0.01, 1.10 ± 0.02, and 5.74 ± 0.74 M^{-1} s^{-1} for cyclohexene, cyclohexen-1-ol, and indene, respectively. A $k(\alpha,\alpha'\text{-}H_4)/k(\alpha,\alpha'\text{-}D_4)$ kinetic isotope effect of 21 ± 1 is observed for the oxidation of cyclohexene. At a 2:1 ratio of $Ru^{IV}{=}O^{2+}$ to olefin, the reactions of $Ru^{IV}{=}O^{2+}$ with either cyclohexene or indene give $Ru^{II}{-}NCCH_3^{2+}$ and the 4-electron ketone products, 2-cyclohexen-1-one and indenone, respectively, as identified by GC−MS. As the ratio of cyclohexene to $Ru^{IV}{=}O^{2+}$ is increased, cyclohexen-1-ol becomes an increasingly competitive product. The mechanisms of these reactions are highly complex. They involve two distinct stages and the formation and subsequent reactions of Ru^{III}-substrate bound intermediates.

Introduction

The results of a variety of studies on the oxidation of cyclohexene by transition metal complexes have been reported in the literature. Oxidation by cytochrome P-450 gives cyclohexene oxide and 2-cyclohexen-1-ol as products.[1] Similar results have been found for model systems based on metalloporphyrins of Fe,[2] Mn,[3] and Cr[4] with iodosylbenzene as the source of the oxidative equivalents. Cyclohexene is also oxidized by high oxidation state complexes of Cu,[5] Mo,[6] V,[7] and Ti.[8] Metalloporphyrins have been used as catalysts for the radical autoxidation of cyclohexene by O_2 giving 2-cyclohexen-1-one as the primary product, but typically after long induction periods.[9a−c] Tabushi and co-workers showed that the autoxidation of cyclohexene catalyzed by manganese tetraphenylporphyrin chloride (Mn^{III}TPPCl) can be significantly promoted by the presence of reducing agents.[9d,e] Mn^{III}TPPCl efficiently catalyzes the autoxidation of cyclohexene to 2-cyclohexen-1-one but in the presence of $NaBH_4$ or H_2 and colloidal platinum, the primary products are cyclohexanol and cyclohexene oxide, respectively. The cyclohexanol formed in the reaction with $NaBH_4$ is most likely due to the reduction of cyclohexene oxide formed as the initial product.

The oxidation of cyclohexene by Cr(V)-oxo heteropolytungstate anions gives both epoxidation and allylic oxidation products. The product ratios can be varied by changing the solvent, the polytungstate ligand, and the countercation.[10] The reaction has been proposed to proceed by radical intermediates.

A magnesium oxide supported polysilazane ruthenium complex is capable of catalyzing the oxygenation of indene to indenone without byproducts under mild conditions. The supported ruthenium complex is also effective without the presence of a cocatalyst.[11]

In earlier work, we showed that *cis*-$[Ru^{IV}(bpy)_2(py)(O)]^{2+}$ oxidizes *trans*-stilbene, *cis*-stilbene, styrene, and norbornene to the corresponding epoxides in CH_3CN.[12] For olefins containing α-C−H bonds, allylic oxidation to the α-ketone occurs in ace-

[†] Current address: Birmingham-Southern College, Box 549022, Arkadelphia Road, Birmingham, AL 35254.

[||] Current address: Los Alamos National Laboratory, Chemistry Division J514, Los Alamos, NM 87545.

[‡] Current address: Spectrum Software Associates, P.O. Box 4494, Chapel Hill, NC 27515-4494. Telephone/Fax: 1-919-942-4061. E-mail: specsoft@compuserve.com.

[§] Current address: Los Alamos National Laboratory, ALDSSR MS A127, Los Alamos, NM 87545. Telephone: 1-505-667-8597. Fax: 1-505-667-5450. E-mail: tjmeyer@lanl.gov.

(1) Groves, J. T.; Krishnan, S.; Avaria, G. E.; Nemo, T. E. In *Biomimetic Chemistry*; Dolphin, D., McKenna, C., Murakami, Y., Tabushi, I., Eds; Advances in Chemistry Series 191; American Chemical Society: Washington, DC, 1980; Chapter 15.

(2) Groves, J. T.; Kruper, W. J.; Nemo, T. E.; Myers, R. S. *J. Mol. Catal.* **1980**, *7*, 169. (b) Medina, J. C.; Gabriunas, N.; PaezMozo, E. *J. Mol. Catal. A-Chem.* **1997**, *115(2)*, 233. (c) Lei, Z. Q. *React. Funct. Polym.* **1999**, *39(3)*, 239.

(3) Nappa, M. J.; McKinney, R. J. *Inorg. Chem.* **1988**, *27*, 3740. (b) KnopsGerrits, P. P.; Vankelecom, I. J. F.; Beatse, E.; Jacobs, P. A. *Catal. Today* **1996**, *32(1−4)*, 63. (c) Matsushita, T.; Sawyer, D. T.; Sobkowiak, A. *J. Mol. Catal. A: Chem.* **1999**, *137(1−3)*, 127.

(4) Garrison, J. M.; Bruice, T. C. *J. Am. Chem. Soc.* **1989**, *111*, 191. (b) Agarwal, D. D.; Goswami, H. S. (c) Agarwal, D. D.; Goswami, H. S.; Raina, D.; Agarwal, S. C. *Ind. J. Chem. B* **1995**, *34(4)*, 357.

(5) Zakharov, A. N.; Zefirov, N. S. *Kinet. Catal.* **1998**, *39(4)*, 493. (b) Kim, Y.; Kim, H.; Lee, J.; Sim, K.; Han, Y.; Paik, H. *Appl. Catal., A* **1997**, *155(1)*, 15.

(6) Olason, G.; Sherrington, D. C. *Macromol. Symp.* **1998**, *131*, 127.

(7) Bahranowski, K.; Kooli, F.; Poltowicz, J.; Serwicka, E. M. *React. Kinet. Catal.* **1998**, *L64(1)*, 3. (b) Schuchardt, U.; Guerreiro, M. C.; Shul'pin, G. B. *Russ. Chem. Bull.* **1998**, *47(2)*, 247.

(8) Chen, L. Y.; Chuah, G. K.; Jaenicke, S. *Catal. Lett.* **1998**, *50(1−2)*, 107. (b) Talsi, E. P.; Shalyaev, K. V. *J. Mol. Catal. A: Chem.* **1996**, *105(3)*, 131. (c) Jappar, N.; Xia, Q. H.; Tatsumi, T. *J. Catal.* **1998**, *180(2)*, 132.

(9) Modnicka, T. In *Metalloporphyrins in Catalytic Oxidations*; Sheldon, R. A., Ed.; Marcel Dekker: New York, 1994, Chapter 9. (b) Paulson, D. R.; Ullman, R.; Sloanne, R. B.; Closs, G. L. *J. Chem. Soc., Chem. Commun.* **1974**, 186. (c) Peterson, M. W.; Rivers, D. S.; Richman, R. M. *J. Am. Chem. Soc.* **1985**, *107*, 2907. (d) Tabushi, I.; Koga, N. *J. Am. Chem. Soc.* **1979**, *101*, 6456. (e) Tabushi, I.; Yazaki, A. *J. Am. Chem. Soc.* **1981**, *103*, 7371.

(10) Khenkin, A. M.; Hill, C. L. *J. Am. Chem. Soc.* **1993**, *115*, 8179.

(11) Wang, T. J.; Sun, F. Y.; Huang, M. Y.; Jiang, Y. Y. *React. Kinet. Catal. Lett.* **1996**, *57(1)*, 147. (b) Hatsuit, T. H. *Bull. Chem. Soc. Jpn.* **1980**, *53(9)*, 2655.

(12) Stultz, L. K.; Binstead, R. A.; Reynolds, M. S.; Meyer, T. J. *J. Am. Chem. Soc.* **1995**, *117*, 2520.

10.1021/ja991722x CCC: $19.00
Published on Web 06/10/2000

tonitrile, as reported for cyclohexene in an earlier work (eq 1).[13] Leising and Takeuchi also reported the catalytic, aerobic oxidation of cyclohexene by *cis*-$[Ru^{II}(bpy)_2(PPh_3)(H_2O)]^{2+}$ which yields 2-cyclohexen-1-one, 2-cyclohexen-1-ol, and small amounts of cyclohexene oxide.[14]

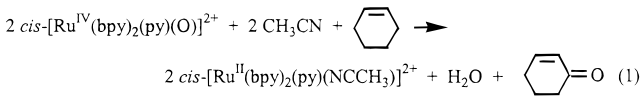

We report here the results of a detailed mechanistic study on the oxidations of cyclohexene and indene by *cis*-$[Ru^{IV}(bpy)_2(py)(O)]^{2+}$. By the use of a combination of UV−visible and FTIR measurements with the application of global analysis, we have been able to identify key intermediates and to demonstrate that these reactions occur by mechanisms which involve a complicated series of kinetically coupled reactions.

For convenience, the following abbreviations will be used throughout the manuscript:

$$cis\text{-}[Ru^{II}(bpy)_2(py)(H_2O)]^{2+} = Ru^{II}\text{−}OH_2{}^{2+}$$

$$cis\text{-}[Ru^{II}(bpy)_2(py)(NCCH_3)]^{2+} = Ru^{II}\text{−}NCCH_3{}^{2+}$$

$$cis\text{-}[Ru^{III}(bpy)_2(py)(OH)]^{2+} = Ru^{III}\text{−}OH^{2+}$$

$$cis\text{-}[Ru^{IV}(bpy)_2(py)(O)]^{2+} = Ru^{IV}{=}O^{2+}$$

$$cis\text{-}[Ru^{IV}(bpy)_2(py)(^{18}O)]^{2+} = Ru^{IV}{=}{}^{18}O^{2+}$$

Experimental Section

Materials. High purity acetonitrile was used as received from Burdick & Jackson. House-distilled water was purified by the use of a Barnstead E-Pure deionization system. High purity NMR solvents and ^{18}O-enriched water were purchased from Cambridge Isotope Laboratories and used as received. Cyclohexene was purified by passage through a column of alumina to remove the BHT stabilizer followed by fractional distillation. 3,3,6,6-tetradeuterocyclohexene was purchased from MSD Isotopes and passed through a plug of powdered alumina immediately prior to use. Common laboratory chemicals employed in the preparation of compounds were reagent grade and used without further purification.

Preparations. The salts *cis*-$[Ru(bpy)_2(py)(O)](PF_6)_2$[15] and *cis*-$[Ru(bpy)_2(py)(^{18}O)](ClO_4)_2$[12] were prepared by literature methods. *Caution!* Although the preparation of the perchlorate salt has been repeated numerous times without incident, particular care should be exercised in its preparation and handling. Perchlorate salts of organometallic cations, metal complexes, and organic cations have been known to explode spontaneously. Hexafluorophosphate was used as the counteranion except when solubility required the use of the perchlorate salt.

Instrumentation. Organic products from the oxidation reactions were analyzed by the use of a Hewlett-Packard 5890 series II gas chromatograph with a 12 m × 0.2 mm × 0.33 μm HP-1 column (cross-linked methyl silicone gum) and a Hewlett-Packard 5971A mass selective detector, both interfaced with an HP Vectra PC computer system. IR spectra were recorded by use of a Mattson Galaxy 5020 series FT-IR spectrophotometer interfaced with an IBM-compatible PC. IR measurements were made either in KBr pellets or in CD_3CN solution by the use of a demountable cell with NaCl plates and Teflon spacers. Kinetic studies with this cell were performed with a manually operated mixing apparatus consisting of Hamilton gastight syringes and a T-valve mixer connected to the solution IR cell with PTFE tubing.

UV−visible spectra were collected as a function of time by the use of a Hewlett-Packard 8452A diode array spectrophotometer interfaced with an IBM-compatible PC. The measurements were made in standard quartz cuvettes or in a solution IR cell (see above) when short path lengths were required. The temperature of solutions during kinetic studies was maintained to within ± 0.2 °C with use of a Lauda RM6 circulating water bath and monitored with an Omega HH-51 thermocouple probe. For rapid reactions, UV−visible spectral changes were followed by use of an OLIS (Bogart, GA) RSM/1000 rapid-scanning, dual beam spectrophotometer linked by liquid light guide to a Hi-Tech Scientific (Salisbury, England) SF-61MX stopped-flow mixing apparatus. Some experiments were performed by use of a Hi-Tech Scientific SF-51 stopped-flow apparatus linked by fiber-optic coupling to either a Beckman DU or a Harrick rapid scan monochromator interfaced with a Zenith 158 computer system employing OLIS data acquisition hardware and software. The temperature of the reactant solutions was controlled to within ±0.2 °C by use of a Neslab RTE−110 water bath and monitored via the Pt resistance thermometers of the SF-51 or SF-61MX mixing units.

Table 1. Pseudo-First-Order Rate Constants for the Oxidation of Cyclohexene by 1.7×10^{-4} M *cis*-$[Ru(bpy)_2(py)(O)]^{2+}$ in CH_3CN at $T = 25.0 \pm 0.1$ °C

[cyclohexene] M	k_{obs} (s^{-1})[a]
2.04×10^{-2}	$(1.35 \pm 0.02) \times 10^{-2}$
4.09×10^{-2}	$(2.53 \pm 0.03) \times 10^{-2}$
6.13×10^{-2}	$(3.71 \pm 0.05) \times 10^{-2}$
8.17×10^{-2}	$(5.14 \pm 0.03) \times 10^{-2}$
1.02×10^{-1}	$(6.50 \pm 0.04) \times 10^{-2}$
1.23×10^{-1}	$(7.71 \pm 0.06) \times 10^{-2}$
1.43×10^{-1}	$(8.76 \pm 0.04) \times 10^{-2}$
1.64×10^{-1}	$(1.02 \pm 0.02) \times 10^{-1}$
1.84×10^{-1}	$(1.16 \pm 0.03) \times 10^{-1}$
2.04×10^{-1}	$(1.28 \pm 0.03) \times 10^{-1}$

[a] Calculated as $k_{obs} = 4 \times k_1$[olefin], $k_1 = 0.16 \pm 0.01$ M^{-1} s^{-1}.

UV−visible Kinetic Studies. All kinetic studies were performed in acetonitrile solution at $T = 25.0 \pm 0.2$ °C, generally with a pseudo-first-order excess of the organic substrate. The concentrations of $Ru^{IV}{=}O^{2+}$ were varied from 4.0×10^{-6} M to 9.4×10^{-3} M with use of 0.020 to 10 cm path length cells in order to maintain absorbance readings within an appropriate range. The concentrations of substrate were varied from 2.04×10^{-2} to 2.04×10^{-1} M for cyclohexene (Table 1), 5.0×10^{-3} to 1.0 M for 2-cyclohexen-1-ol, and 0.010 to 0.200 M for indene.

The presence of intermediates in the reactions of $Ru^{IV}{=}O^{2+}$ with the olefins was investigated by monitoring the UV−visible spectral changes after quenching reaction mixtures at various times by the addition of a small excess of either hydroquinone or ascorbic acid. Both reductants rapidly reduce all Ru(IV) or Ru(III) species to their Ru(II) forms, which are more easily detected by their characteristic MLCT absorption bands[16] and their different rates of solvolysis to $Ru^{II}\text{−}NCCH_3{}^{2+}$.

Multi-wavelength kinetic data were processed by the use of the program SPECFIT.[17] When necessary, the program was used with molar absorptivity spectra of known species and/or known rate constants to constrain the global least-squares fit. A more detailed description of the global kinetic analysis is given in an earlier publication.[16] Single wavelength data were analyzed with the program KINFIT.[18]

Results

Organic Product Analysis and Stoichiometry. Organic products from the reactions between $Ru^{IV}{=}O^{2+}$ and cyclohexene

(13) Seok, W. K.; Dobson, J. C.; Meyer, T. J. *Inorg. Chem.* **1988**, *27*, 5. (b) Kanmani, A. S.; Vancheesan, S. *J. Mol. Catal. A: Chem.* **1997**, *125(2−3)*, 127. (c) Cheng, W. C.; Yu, W. Y.; Li, C. K.; Che, C. M. *J. Org. Chem.* **1995**, *60(21)*, 6840.

(14) Leising, R. A.; Takeuchi, K. J. *Inorg. Chem.* **1987**, *26*, 4391.

(15) Moyer, B. A.; Meyer, T. J. *Inorg. Chem.* **1981**, *20*, 436.

(16) Binstead, R. A.; Stultz, L. K.; Meyer, T. J. *Inorg. Chem.* **1995**, *34*, 546.

(17) *SPECFIT*, Spectrum Software Associates: Chapel Hill, NC, 1995.

(18) Binstead, R. A. *KINIFT*, Nonlinear Curve Fitting for Kinetic Systems; Chemistry Department: University of North Carolina, Chapel Hill, NC, 1990.

Table 2. Product Analyses by GC−MS for Cyclohexene and Indene Oxidation by *cis*-$[Ru^{IV}(bpy)_2(py)(O)]^{2+}$ in CH_3CN at $T = 25 \pm 1$ °C

reaction[a]	$Ru^{IV}{=}O^{2+}$:olefin	products	fractional yield[b]
$Ru^{IV}{=}O^{2+}$ + cyclohexene	2:1	2-cyclohexen-1-ol	8
		2-cyclohexen-1-one	92
	2:1.5	2-cyclohexen-1-ol	14
		2-cyclohexen-1-one	86
	1:5	2-cyclohexen-1-ol	37
		2-cyclohexen-1-one	63
	1:25	2-cyclohexen-1-ol	51
		2-cyclohexen-1-one	49
	1:50	2-cyclohexen-1-ol	53
		2-cyclohexen-1-one	47
$Ru^{IV}{=}O^{2+}$ + indene	2:1	indene	9[c]
		indenone	91
	1:1	indene	55[c]
		indenone	45
	1:2	indene	80[c]
		indenone	20

[a] *cis*-$[Ru(bpy)_2(py)(O)]^{2+} = 6.5$ mM for cyclohexene oxidation and 15 mM for indene oxidation. [b] The total product yield was 93−96% based on added $Ru^{IV}{=}O^{2+}$. [c] The ratio of unreacted indene to indenone.

or indene in CH_3CN under argon were determined by GC−MS analysis of mixtures obtained after reaction times of 2−24 h at room temperature. Calibration curves and product analyses for the oxidation of cyclohexene are provided in Supporting Information Figures S1 and S2. The product distributions obtained at $Ru^{IV}{=}O^{2+}$ to olefin ratios of 2:1, 1:1.5, 1:5, 1:25, and 1:50 are listed in Table 2. For cyclohexene oxidation, the total yields for organic products were 93−96% based on $Ru^{IV}{=}{}^{16}O^{2+}$ added.

The oxidation of indene yielded only the 4-electron allylic product, indenone. On the basis of oxidation by 2 equiv of $Ru^{IV}{=}O^{2+}$, indenone was formed in ∼90% yield. The corresponding allylic alcohol and epoxide products were not detected by GC−MS analysis, even with a 50:1 ratio of indene to $Ru^{IV}{=}O^{2+}$.

In the oxidation of cyclohexene by $Ru^{IV}{=}O^{2+}$, both the allylic alcohol, 2-cyclohexen-1-ol, and allylic ketone, 2-cyclohexen-1-one, were detected. At a 2:1 ratio of $Ru^{IV}{=}O^{2+}$ to cyclohexene, only 8% of the alcohol was formed, but as the ratio of substrate to oxidant was increased, the proportion of alcohol increased. When the reaction was performed with a 50-fold excess of cyclohexene, the percentage yield of the alcohol product rose to 53%. Epoxide products were not observed in any of the GC−MS product analyses. Further experimental details are given in Supporting Information.

^{18}O-Labeling Studies. ^{18}O-labeling experiments were conducted in CH_3CN. In these experiments, cyclohexene and indene were oxidized by $Ru^{IV}{=}{}^{18}O^{2+}$ and the products determined by both FTIR spectroscopy and GC−MS analysis. The results of the GC−MS analyses are summarized in Table 3.

The ^{18}O-labeling study for the oxidation of cyclohexene was performed at a 1:5 ratio of $Ru^{IV}{=}{}^{18}O^{2+}$ to cyclohexene. Under these conditions, both 2-cyclohexen-1-one and 2-cyclohexen-1-ol are products. None of the alcohol product was ^{18}O-labeled, while 2-cyclohexen-1-one was found to be 61 ± 15% labeled, as shown by FTIR band intensity measurements. With the ^{18}O label, ν(C=O) in the cyclohexenone product shifted to 1685 cm^{-1} from 1648 cm^{-1} in the ^{18}O product. Baseline inconsistencies and overlap with nearby bands limited the accuracy of the analysis. Oxidation of indene by $Ru^{IV}{=}{}^{18}O^{2+}$ at a 1:1 ratio gave 80 ± 5% ^{18}O incorporation into the indenone product by GC−MS analysis. When the same reaction was studied by FTIR, ν(C=O) in the product shifted from 1712 cm^{-1} (^{16}O) to 1684 cm^{-1} (^{18}O).

Table 3. Results of Isotope Labeling for Olefin Oxidations by *cis*-$[Ru(bpy)_2(py)(O)]^2$ in CH_3CN at $T = 25 \pm 1$ °C by GC−MS

reaction[a]	stoichiometry	product	fractional yield
$Ru^{IV}{=}O^{2+}$ + d_4-cyclohexene	2:1	d_2-cyclohexenone	98
		d_3-cyclohexenone	2
	1:1	d_2-cyclohexenone	95
		d_3-cyclohexenone	5
	1:2	d_2-cyclohexenone	80
		d_3-cyclohexenone	20
$Ru^{IV}{=}{}^{18}O^{2+}$ + cyclohexene	1:5	^{16}O-cyclohexenol	14
		^{18}O-cyclohexenol	0
		^{16}O-cyclohexenone	25
		^{18}O-cyclohexenone	61
$Ru^{IV}{=}O^{2+}$ + cyclohexene + $H_2{}^{18}O$[b]	1:1	^{16}O-cyclohexenol	7
		^{18}O-cyclohexenol	0
		^{16}O-cyclohexenone	89
		^{18}O-cyclohexenone	4
$Ru^{IV}{=}{}^{18}O^{2+}$ + indene	1:1	^{16}O-indenone	20
		^{18}O-indenone	80
$Ru^{IV}{=}O^{2+}$ + indene + $H_2{}^{18}O$[b]	1:1	^{16}O-indenone	97
		^{18}O-indenone	3

[a] $[Ru^{IV}{=}O^{2+}] = 15$ mM. [b] CH_3CN solvent 2% v/v in $H_2{}^{18}O$.

Scheme 1

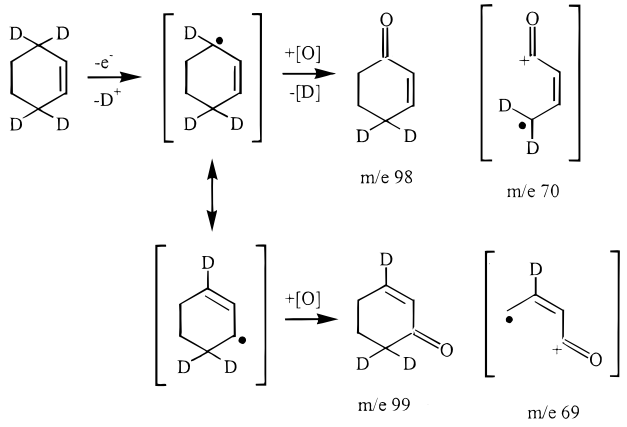

The oxidations of cyclohexene and indene by $Ru^{IV}{=}{}^{16}O^{2+}$ were also performed in CH_3CN containing 2% v/v $H_2{}^{18}O$, and the products were analyzed by GC−MS. The 2-cyclohexen-1-ol product contained no ^{18}O label, while 2-cyclohexen-1-one was 4% ^{18}O-labeled. Similarly in the oxidation of indene, only 3% of the indenone produced contained the ^{18}O label.

Oxidation of 3,3,6,6-Tetradeuterocyclohexene. Oxidation of 3,3,6,6-tetradeuterocyclohexene (d_4-cyclohexene) was investigated as a probe for possible radical intermediates. As illustrated in Scheme 1, radical formation followed by allylic rearrangement[19] would lead to inequivalent ketone products, one containing two deuteriums having molecular weight 98 amu and the other containing three deuteriums having molecular weight 99 amu. Allylic rearrangement can be distinguished by the appearance of parent ions at *m*/*e* ratios of 98 and 99, and parent minus ethylene at 69 and 70 with correction for ^{13}C. Results at ratios of $Ru^{IV}{=}O^{2+}$ to cyclohexene of 2:1, 1:1, and 1:2 are listed in Table 3. From these data, it is evident that at a 2:1 ratio of $Ru^{IV}{=}O^{2+}$ to cyclohexene, only 2% of the ketone product underwent allylic rearrangement, while at a 1:2 ratio, the amount of rearranged ketone increased to 20%.

(19) Groves, J. T.; Subramanian, D. V. *J. Am. Chem. Soc.* **1984**, *106*, 2177.

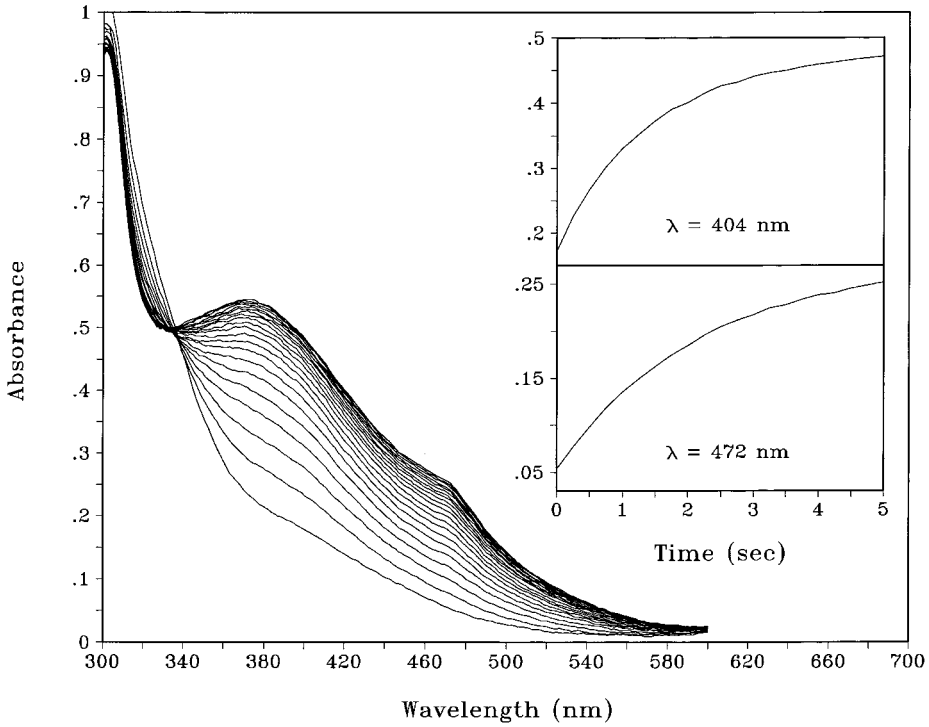

Figure 1. Rapid-scan stopped-flow, UV−visible spectral changes for the reaction between 1.0×10^{-4} M *cis*-$[Ru^{IV}(bpy)_2(py)(O)]^{2+}$ and 1.0 M cyclohexene in CH_3CN at $T = 25.0 \pm 0.2$ °C, path length = 1.0 cm, $0 < t < 5$ s.

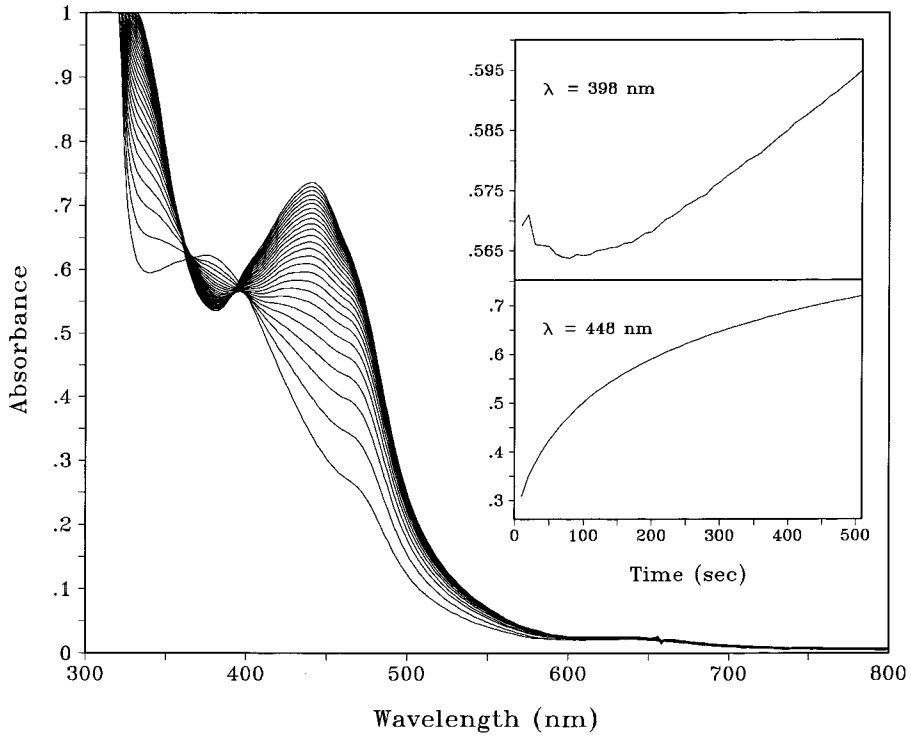

Figure 2. Diode array, UV−visible spectral changes with manual mixing for the reaction between 1.0×10^{-4} M *cis*-$[Ru^{IV}(bpy)_2(py)(O)]^{2+}$ and 1.0 M cyclohexene in CH_3CN at $T = 25.0 \pm 0.2$ °C, path length = 1.0 cm, $0 < t < 5$ s.

Spectral Changes during the Oxidation of Cyclohexene. In Figure 1 are shown UV−visible spectral changes that occur during the initial stage of the oxidation of cyclohexene (1.0 M) by $Ru^{IV}{=}O^{2+}$ (1.0×10^{-4} M). In the first 5 s after stopped-flow mixing, the initial spectrum of $Ru^{IV}{=}O^{2+}$ was replaced by a spectrum characteristic of $Ru^{III}{-}OH^{2+}$ ($\lambda_{max} = 380$ nm, $\epsilon = 5520$ M^{-1} cm^{-1}).[16] A small shoulder also appeared at ~470 nm consistent with the MLCT band for $Ru^{II}{-}OH_2^{2+}$ ($\lambda_{max} =$ 468 nm, $\epsilon = 8750$ M^{-1} cm^{-1}).[16] Spectral changes collected on a diode array spectrophotometer after manual mixing are shown in Figure 2. In the time required to mix the reactants in the cell (5−10 s), the first stage of the reaction was nearly complete. In the second stage of the reaction, shown in Figure 2, the absorbance at 380 nm decreased, while the absorbance at 440 nm increased. The final trace corresponds to the spectrum of $Ru^{II}{-}NCCH_3^{2+}$ ($\lambda_{max} = 440$ nm, $\epsilon = 8160$ M^{-1} cm^{-1}).[16]

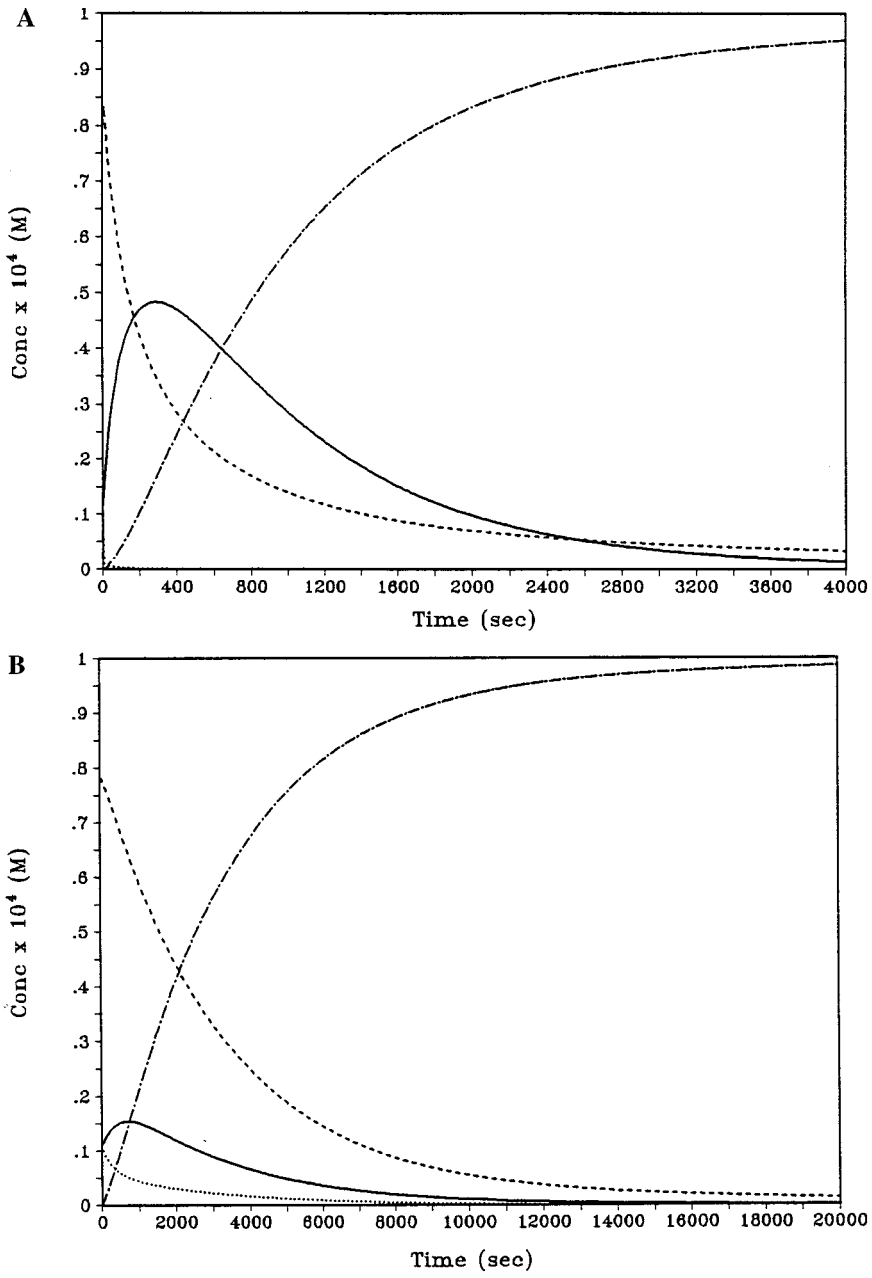

Figure 3. Predicted concentration profiles determined by kinetic simulation of the disproportionation of $Ru^{III}-OH^{2+}$ followed by $Ru^{IV}=O^{2+}$ oxidation in the presence of (a) 1 M cyclohexene and (b) 0.01 M cyclohexene, $Ru^{IV}=O^{2+}$ (···), $Ru^{III}-OH^{2+}$ (- - -), $Ru^{II}-OH_2^{2+}$ (—), $Ru^{II}-NCCH_3^{2+}$ (— · —).

The nature of the products of the initial stage ($t \approx 10$ s) was investigated further by a series of quenching experiments in which an excess of hydroquinone was added to reduce Ru(IV) and Ru(III) to Ru(II) (Supporting Information Figure S3). Singular value decomposition (SVD) of the spectral data after quenching indicated the presence of three predominant colored components and two distinct kinetic processes both leading to $Ru^{II}-NCCH_3^{2+}$. A global fit of the data to the biexponential model, A → C, B → C (k_A and k_B are the rate constants for the two steps) gave $k_A = (1.28 \pm 0.04) \times 10^{-2}$ s^{-1} and $k_B = (1.46 \pm 0.02) \times 10^{-3}$ s^{-1}. The latter is consistent with k for solvolysis of $Ru^{II}-OH_2^{2+}$ in 1 M cyclohexene/CH_3CN, $k_{solv} = (1.48 \pm 0.02) \times 10^{-3}$ s^{-1}, $T = 25.0 \pm 0.2$ °C. The total concentration of Ru was adjusted from the predicted spectrum of the final product C to obtain the correct molar absorptivity for $Ru^{II}-NCCH_3^{2+}$. With B identified as $Ru^{II}-OH_2^{2+}$, the initial concentrations were adjusted so that the predicted spectrum of B matched that of $Ru^{II}-OH_2^{2+}$. The resulting global fit returned the predicted spectrum of A, a Ru(II) intermediate that undergoes solvolysis more rapidly than $Ru^{II}-OH_2^{2+}$ (Supporting Information Figure S4). On the basis of this analysis, [A]:[$Ru^{II}-OH_2^{2+}$] ≈ 1:5 although this ratio includes the small amount of $Ru^{II}-OH_2$ present before the addition of hydroquinone.

The nature of the bound intermediate was investigated by GC−MS analysis of reaction mixtures after quenching. With cyclohexene at 1.1×10^{-2} M and $Ru^{IV}=O^{2+}$ at 2.3×10^{-3} M, hydroquinone 2.7×10^{-2} M was added after 1 min, and the initial products allowed to solvolyze for an additional 30 min. 2-cyclohexen-1-one, benzoquinone, and hydroquinone were detected by GC−MS. No 2-cyclohexen-1-ol was detected initially, but it did appear as a product over time. Quenching after 5 min gave a [ketone]:[alcohol] ratio of 6:1.

The kinetics of the initial stage in the oxidation of cyclohexene by $Ru^{IV}=O^{2+}$ (1.7×10^{-4} M) were investigated under pseudo first-order conditions with a large excess of olefin ($2.04 \times 10^{-2} - 2.04 \times 10^{-1}$ M). Single wavelength measurements

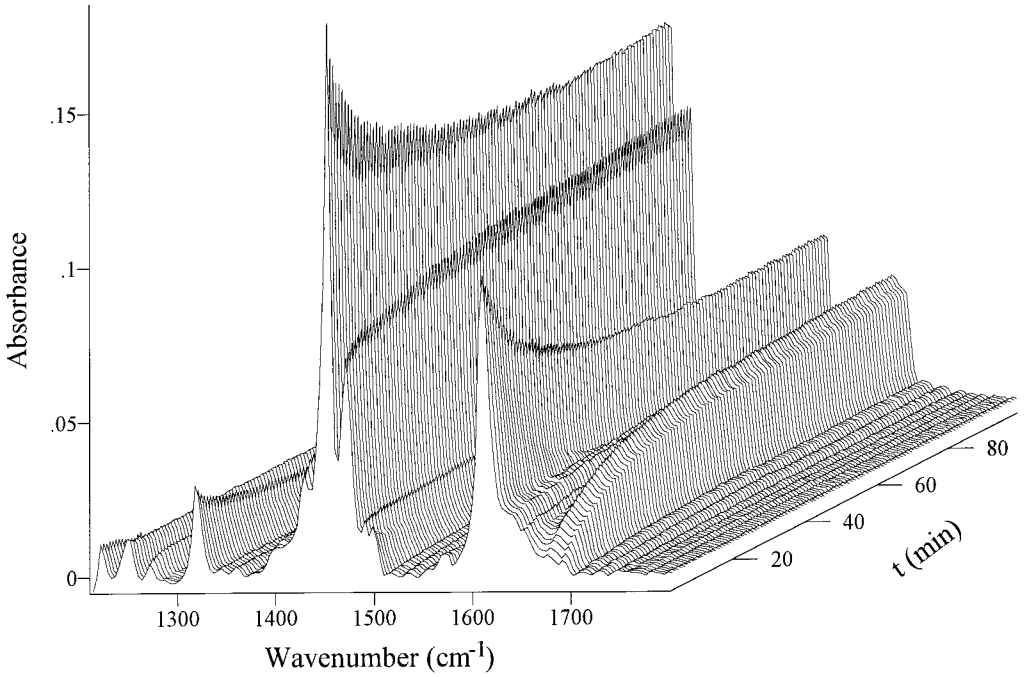

Figure 4. IR spectral changes for the reaction between 7.6×10^{-3} M *cis*-$Ru^{IV}(bpy)_2(py)(O)]^{2+}$ and 2.78×10^{-2} M cyclohexene in CD_3CN, path length = 0.2 mm (NaCl).

at 388−400 nm were fit to pseudo-first-order kinetics. The experimental rate constant, k_{obs}, was found to vary linearly with olefin concentration, and matched well with studies performed at 1.0 M added olefin.

The spectral changes in Figure 1 show that Ru(IV) is reduced to Ru(III) in the first step. The presence of ketone in the reaction mixture after quenching shows that more than two oxidative equivalents per olefin are consumed. This demonstrates that the mechanism is complex and does not involve a single kinetic process. This conclusion is supported by the appearance of both $Ru^{II}-OH_2^{2+}$ and a second Ru(II) intermediate after hydroquinone quenching.

On the basis of this analysis, the interpretation of k_{obs} and its olefin dependence must include both rate-determining oxidation of cyclohexene and following steps in which further oxidation by $Ru^{IV}=O^{2+}$ occurs. The rate constant for the rate-determining step, k', can be calculated from eq 2

$$k' = \frac{k_{obs}}{n[\text{olefin}]} \qquad (2)$$

in which n is the stoichiometry of $Ru^{IV}=O^{2+}$ consumed in the initial stage. For cyclohexene, the value $n = 4$ was used to calculate k' based on the analysis in Discussion.

The quenching studies demonstrate that there are two forms of Ru(III) after the initial stage but predominantly $Ru^{III}-OH^{2+}$. The slower spectral changes that occur past 10 s (Figure 2) can be accounted for largely by a mechanism involving: (1) initial disproportionation of $Ru^{III}-OH^{2+}$,

$$2\ Ru^{III}-OH^{2+} \underset{4070\ M^{-1}\ s^{-1}}{\overset{81\ M^{-1}\ s^{-1}}{\rightleftharpoons}} Ru^{IV}=O^{2+} + Ru^{II}-OH_2^{2+} \qquad (3)$$
$$(K = 0.02)$$

(2) further oxidation of cyclohexene by $Ru^{IV}=O^{2+}$; and, (3) solvolysis of $Ru^{II}-OH_2^{2+}$. Concentration profiles calculated by kinetic simulation of this mechanism in the presence of 1 and 0.01 M cyclohexene are shown in Figure 3.

Although this mechanism fits the absorbance-time traces reasonably well, it is incomplete. It does not account for the fact that 2-cyclohexen-1-ol becomes an increasingly important product as the $Ru^{IV}=O^{2+}$:olefin ratio is increased. It also does not explain how the free ketone product appears in the solution.

The oxidation of 3,3,6,6-tetradeuterocyclohexene by $Ru^{IV}=O^{2+}$ is considerably slower than the oxidation of cyclohexene. UV−visible spectral changes with time are shown in Supporting Information Figures S5 and S6. The reactions were performed with only a 10-fold excess of reductant to guard against possible interference by small amounts of partially deuteriated impurities. For d_4-cyclohexene, the reaction was performed with 1.0×10^{-2} M d_4-cyclohexene and 1.0×10^{-3} M $Ru^{IV}=O^{2+}$ (path length = 0.10 cm) which was compared to the reaction between 1.0×10^{-3} M cyclohexene and 1.0×10^{-4} M $Ru^{IV}=O^{2+}$ (path length = 1.00 cm). In both cases, the UV−visible spectral changes were analyzed with SPECFIT. The SVD analysis of the spectral-time traces indicated the presence of five colored components, but two were present at very low levels. This precluded the use of a complete kinetic model; however, the data could be fit to biexponential kinetics, A → B → C which was adequate to isolate the apparent rate constant for the initial stage. This procedure yielded $k' = (9.75 \pm 0.03) \times 10^{-3}\ M^{-1}\ s^{-1}$ for d_4-cyclohexene, and $k' = 0.20 \pm 0.01\ M^{-1}\ s^{-1}$ for cyclohexene. On the basis of these values, the $k(\alpha,\alpha'\text{-}H_4)/k(\alpha,\alpha'\text{-}D_4)$ kinetic isotope effect is 21 ± 1 for this reaction.

The reaction between cyclohexene and $Ru^{IV}=O^{2+}$ was also monitored by FTIR at ratios of between 2:1 and 1:7 of $Ru^{IV}=O^{2+}$ to cyclohexene. The results of a typical experiment are shown in Figure 4. A series of ν(bpy) ring stretching modes appeared in the region 1300−1600 cm^{-1} that varied in energy and molar absorptivity with oxidation state of the complex. Kinetic analysis of the IR data showed that the initial, rapid stage of the reaction was first-order in both cyclohexene and $Ru^{IV}=O^{2+}$. The latter stages were relatively independent of both. The SVD of the spectral data showed the presence of four contributors. The kinetics could be modeled by the rate

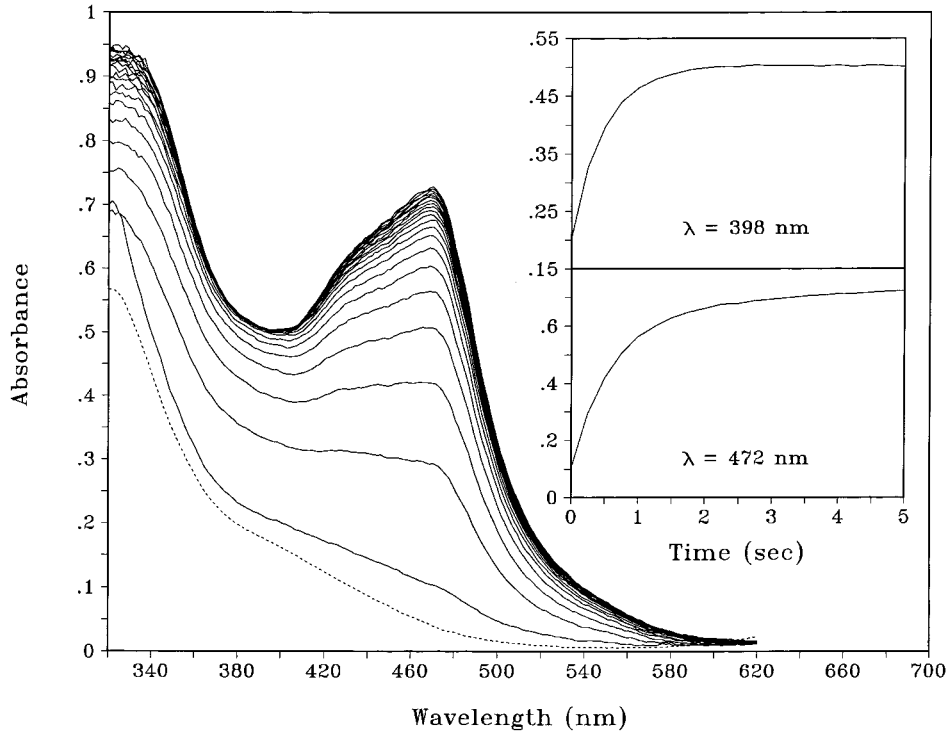

Figure 5. Rapid-scan, UV−visible spectral changes for the reaction between 1.0×10^{-4} M *cis*-$[Ru^{IV}(bpy)_2(py)(O)]^{2+}$ and 1.0 M 2-cyclohexen-1-ol in CH_3CN solution at $T = 25.0 \pm 0.2$ °C, path length = 1.0 cm.

Scheme 2

$$Ru^{IV}{=}O^{2+} + \text{cyclohexenol} \xrightarrow{k_1} Ru^{III}\text{-}OH^{2+} + \text{cyclohexenone} + H^+$$

$$Ru^{III}\text{-}OH^{2+} + H^+ \xrightarrow{\text{rapid}} Ru^{II}\text{-}OH_2{}^{2+}$$

$$Ru^{IV}{=}O^{2+} + Ru^{II}\text{-}OH_2{}^{2+} \underset{81\ M^{-1}\ s^{-1}}{\overset{4070\ M^{-1}\ s^{-1}}{\rightleftharpoons}} 2\ Ru^{III}\text{-}OH^{2+}$$

law (A → B → C → D). While simplified, this model allowed the rate constant for the initial oxidation of cyclohexene by $Ru^{IV}{=}O^{2+}$ to be separated from the following steps. On the basis of this analysis, for the reaction between 2.78×10^{-2} M cyclohexene and 7.6×10^{-3} M $Ru^{IV}{=}O^{2+}$, $k_{obs} = (1.53 \pm 0.08) \times 10^{-2}$ s^{-1} and $k' = 0.138 \pm 0.008$ M^{-1} s^{-1}. These values are consistent with values obtained from UV−visible measurements.

The appearance of the ketone product was monitored by the growth in ν(C=O) at 1685 cm^{-1}. It occurred in the latter stages of the reaction and deviates slightly from single-exponential kinetics. The results of the global fit returned almost identical spectra for species C and D. These observations suggest that the free ketone is released in two separate steps with $k_2 = (1.4 \pm 0.2) \times 10^{-3}$ and $k_3 = (1.7 \pm 0.1) \times 10^{-4}$ s^{-1}.

Spectral Changes for the Oxidation of 2-Cyclohexen-1-ol. The oxidation of 2-cyclohexen-1-ol by $Ru^{IV}{=}O^{2+}$ was studied independently. The spectral changes at early time are shown in Figure 5. The kinetics in this case were highly wavelength dependent. Absorbance changes from of 389−400 nm were used to follow the growth of Ru(III). The data in this region exhibited biexponential kinetics with an approximate ratio of 2:1 for the observed rate constants. This behavior was more pronounced at high concentrations of $Ru^{IV}{=}O^{2+}$ and cyclohexenol. Our observations are consistent with initial 2-electron oxidation of the alcohol followed by comproportionation, as shown in Scheme 2.

Table 4. Rate Constants for the Oxidation of Indene by *cis*-$[Ru^{IV}(bpy)_2(py)(O)]^{2+}$ in CH_3CN at $T = 25.0 \pm 0.2$ °C[a]

indene M	$[Ru^{IV}{=}O^{2+}]$ (M)	k_1 (s^{-1})	k_2 (s^{-1})	k_3 (s^{-1})
0.010	2.0×10^{-5}	0.142 ± 0.009	0.025 ± 0.003	0.012 ± 0.003
0.010	1.0×10^{-4}	0.144 ± 0.002	0.018 ± 0.005	0.004 ± 0.001
0.020	2.0×10^{-5}	0.290 ± 0.020	0.030 ± 0.003	0.011 ± 0.002
0.020	1.0×10^{-4}	0.282 ± 0.008	0.076 ± 0.009	0.015 ± 0.001
0.050	2.0×10^{-5}	0.680 ± 0.020	0.032 ± 0.005	0.010 ± 0.001
0.050	1.0×10^{-4}	0.655 ± 0.006	0.046 ± 0.009	0.008 ± 0.002
0.100	2.0×10^{-5}	1.390 ± 0.060	0.040 ± 0.007	0.010 ± 0.001
0.100	1.0×10^{-4}	1.270 ± 0.010	0.042 ± 0.004	0.008 ± 0.002
0.200	2.0×10^{-5}	2.300 ± 0.100	0.040 ± 0.005	0.009 ± 0.001
0.200	1.0×10^{-4}	2.410 ± 0.050	0.044 ± 0.006	0.008 ± 0.003

[a] The data were fit to the model A → B → C → D → E, with k_1, k_2, k_3, and k_4 = the rate constants for each step from A to E, with SPECFIT. k_4 was fixed at 1.66×10^{-3} s^{-1}, the rate constant for solvolysis of $Ru^{II}{-}OH_2{}^{2+}$ in CH_3CN.

As shown in Supporting Information Figure S7, kinetic simulation with $k_1 = 2$ M^{-1} s^{-1} demonstrated that the growth of $Ru^{III}{-}OH^{2+}$ is biexponential under conditions of high $Ru^{IV}{=}O^{2+}$ (1.0×10^{-4} M) and cyclohexenol (1 M). At lower concentrations, the kinetic behavior is close to exponential. Results are summarized in Table S1. A plot of k_{obs} (s^{-1}) versus the cyclohexenol concentration was linear, and a linear least-squares fit gave $k_{obs} = 2.20 \pm 0.02$ M^{-1} s^{-1} with an intercept of 0.016 ± 0.009 s^{-1}. On the basis of eq 2 with $n = 2$, $k' = 1.10 \pm 0.02$ M^{-1} s^{-1}.

Spectral Changes for the Oxidation of Indene. In Figure 6A are shown UV−visible spectral traces with time for the reaction between $Ru^{IV}{=}O^{2+}$ (9.1×10^{-5} M) and indene (5.04×10^{-2} M) in CH_3CN at 25 °C. At early times ($t < 5$ s), $Ru^{IV}{=}O^{2+}$ disappeared with the concomitant growth of an intermediate with absorption maxima near 380 nm and ~550 nm. The ultimate product was $Ru^{II}{-}NCCH_3{}^{2+}$ ($\lambda_{max} = 440$ nm, $\epsilon = 8160$ M^{-1} s^{-1}).[16]

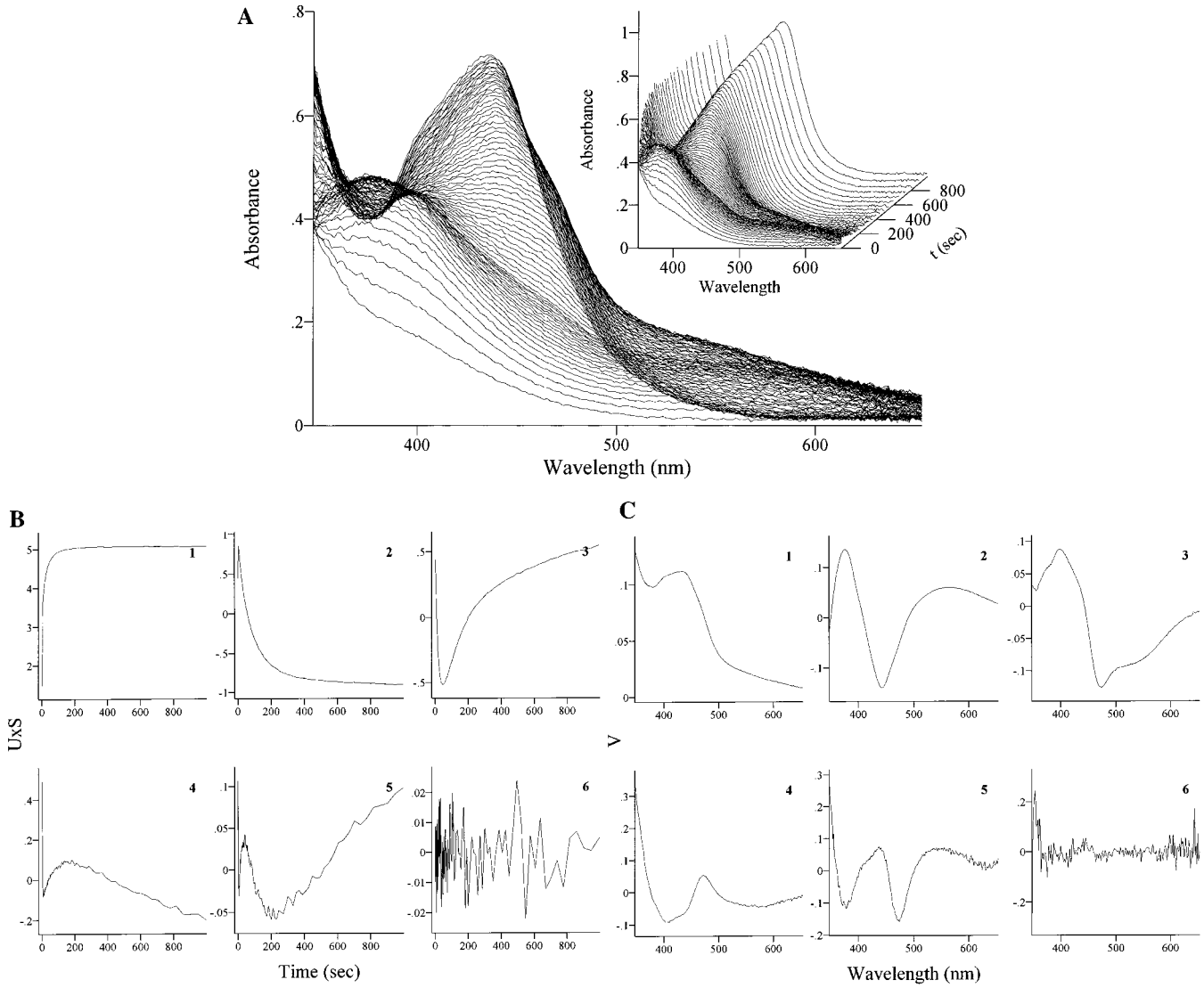

Figure 6. (A) Rapid-scan, UV−vis spectral changes for the reaction between 9.1×10^{-5} M *cis*-$[Ru^{IV}(bpy)_2(py)(O)]^{2+}$ and 0.0504 M indene in CH_3CN at $T = 25.0 \pm 0.2$ °C. Each trace represents the average of 160×1 ms scans. (B) The first six temporal eigenvectors from U × S. (C) First six spectral eigenvectors, V, from the singular value decomposition analysis of the data matrix, Y. By definition, the scan data can be reconstructed as Y = U × S × V.

Singular value decomposition (SVD) of this data set gave evidence for the presence of five distinct contributing components and four-coupled kinetic processes (Figure 6B and C). The kinetics could be modeled by a multi-exponential series consistent with the mechanism A → B → C → D → E, with k_1, k_2, k_3, and k_4 = the rate constants for each step from A to E, A = Ru^{IV}═O^{2+}, and E = Ru^{II}−$NCCH_3^{2+}$. Predicted spectra and concentration profiles from a typical global fit are shown in Figure 7A and B. Observed first-order rate constants for the first three stages were listed in Table 4 as a function of the concentrations of indene and Ru^{IV}═O^{2+}. Since some of the data sets did not extend far enough in time to determine the fourth rate constant uniquely, its value was fixed at 1.66×10^{-3} s^{-1}. This is the rate constant for solvolysis of Ru^{II}−OH_2^{2+}. The rate constants derived from the kinetic fits were the same for data obtained in aerated solutions and under a nitrogen atmosphere.

The observed rate constant (k_{obs}, s^{-1}) for the first step varied linearly with the concentration of indene. A linear least-squares fit to the data yielded the second-order rate constant $k' = 5.74 \pm 0.4$ M^{-1} s^{-1} from the slope by using eq 2 with $n = 2$ (see Discussion). The intercept was near zero (0.07 ± 0.03 s^{-1}).

The predicted spectrum of the product of the first stage (Figure 7A) appeared to be a superposition of Ru^{III}−OH^{2+} and an intermediate with $\lambda_{max} \approx 550$ nm. To determine the nature of the intermediate, the reaction was quenched at this point by addition of either hydroquinone or ascorbic acid as reducing agent (Supporting Information Figure S8). SVD of the spectra after the addition of the reductant indicated the presence of a minimum of four colored components. The most rapid spectral change was dependent on the concentration of added reductant and led to further formation of Ru(II). This arises from reduction of an intermediate since Ru^{III}−OH^{2+} is reduced rapidly by hydroquinone ($k \approx 1 \times 10^6$ M^{-1} s^{-1}) and would not be detectable on this time scale.[20] There must be at least two Ru(II) intermediates, and both undergo solvolysis to give Ru^{II}−$NCCH_3^{2+}$. The first ($\lambda_{max} = 468$ nm, $k_{solv} = (1.56 \pm 0.02) \times 10^{-3}$ s^{-1}) is Ru^{II}−OH_2^{2+} formed by reduction of Ru^{III}−OH^{2+} or unreacted Ru^{IV}═O^{2+}.[18] The second contains either coordi-

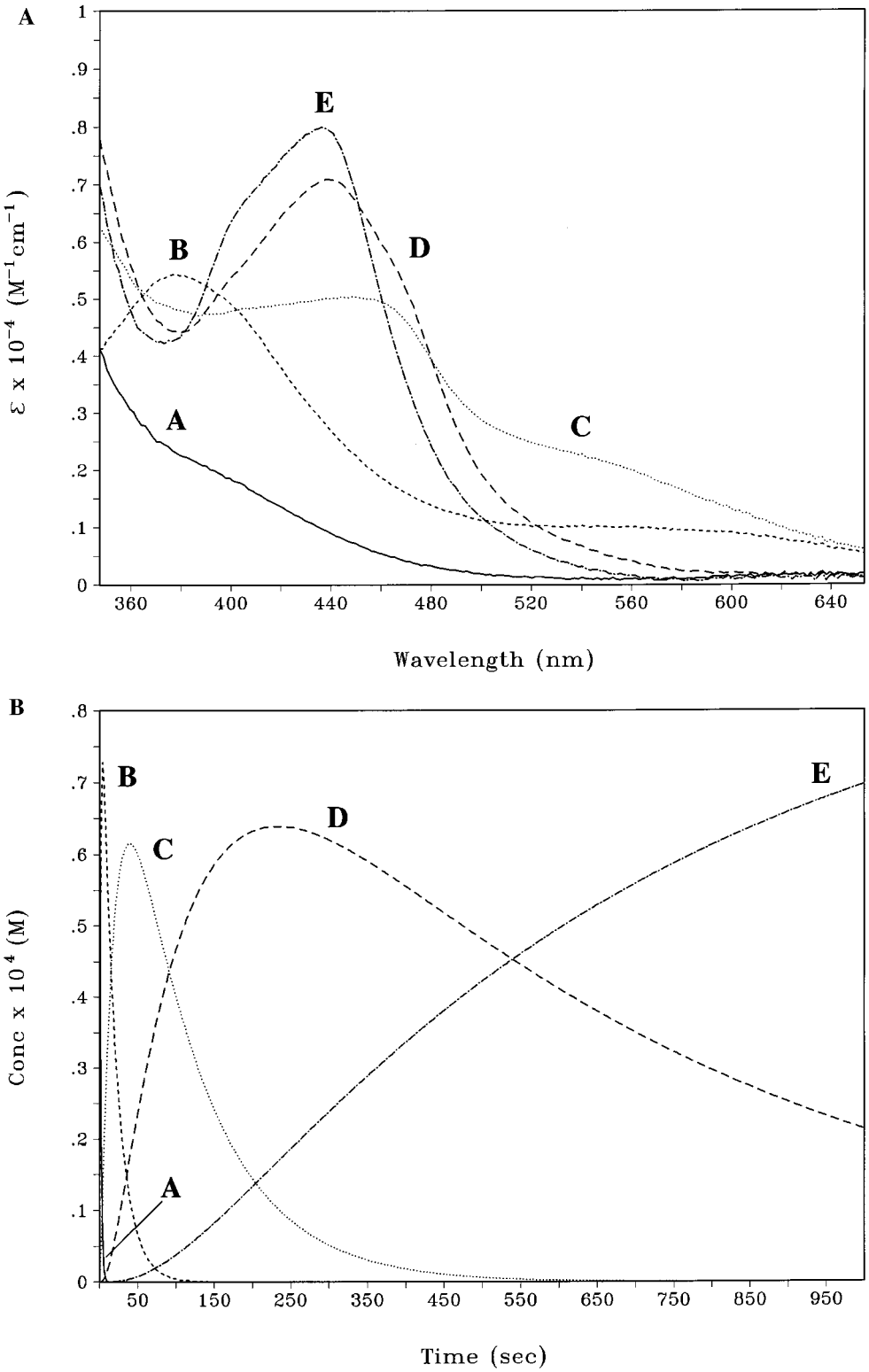

Figure 7. (**A)** Predicted spectra obtained from a global fit of the data in Figure 6A to the multi-exponential kinetic model (A → B → C → D → E). A(—), B(- - -), C(···), D(– – –), E(— · —) with A = Ru^{IV}═O^{2+} and E = Ru^{II}═$NCCH_3^{2+}$. (**B)** As in Figure 7A showing predicted concentration profiles.

nated ketone or alcohol, solvolyzes with $k_{solv} = (2.6 \pm 0.2) \times 10^{-2}$ s^{-1}, and has an MLCT absorption feature at $\lambda_{max} = 550-650$ nm. From the known molar absorptivities of $Ru^{II}-OH_2^{2+}$ and $Ru^{II}-NCCH_3^{2+}$, the ratio of $Ru^{II}-OH_2^{2+}$ to Ru(II) intermediate was ~1.4:1.

In the second stage of the reaction, both Ru(III) intermediates were reduced to Ru(II). The rate constants obtained from the multiexponential fits appeared to be independent of the concentrations of both indene and initially added Ru^{IV}═O^{2+} with $k_2 = 0.042$ s^{-1} (Table 4). k_2 was kinetically well-defined only at relatively high olefin concentrations because of kinetic overlap with the solvolysis steps. The rate constants for the third and

(20) Binstead, R. A.; McGuire, M. E.; Dovletoglou, A.; Seok, W. K.; Roecker, L. E.; Meyer, T. J. *J. Am. Chem. Soc.* **1992**, *114*, 173.

fourth steps were also independent of both indene and $Ru^{IV}{=}O^{2+}$. The latter appeared to involve solvolysis of a Ru(II) intermediate with $k_3 = 0.010 \pm 0.002\ s^{-1}$ and solvolysis of $Ru^{II}{-}OH_2^{2+}$ to give $Ru^{II}{-}NCCH_3^{2+}$.

The oxidation of indene by $Ru^{IV}{=}O^{2+}$ was also monitored by FTIR spectroscopy at ratios of between 2:1 and 1:6 $Ru^{IV}{=}O^{2+}$ to indene at room temperature. ν(Ru=O) at 800 cm^{-1} was absent in even the earliest scans, showing that $Ru^{IV}{=}O^{2+}$ had been consumed by 5−10 s after mixing, consistent with the results of the stopped-flow experiments. The growth of ν(C=O) for the ketone at 1712 cm^{-1} was independent of indene and initial $Ru^{IV}{=}O^{2+}$ with $k_{obs} = (1.2 \pm 0.4) \times 10^{-2}\ s^{-1}$ which coincided with k_3 in the multiexponential fit to the UV−visible data. There was no evidence for ν(C=O) in the intermediate before solvolysis (Supporting Information Figure S9).

Discussion

Unlike cytochrome P-450 and some model porphyrin complexes, epoxides are not observed as products in the oxidations of indene or cyclohexene by $Ru^{IV}{=}O^{2+}$. At least at 25 °C, $Ru^{IV}{=}O^{2+}$ prefers to insert into an allylic C−H bond rather than to add to the double bond of the olefin. Epoxidation is a known reaction for the stilbenes and other olefins where allylic oxidation cannot occur.[12]

For the two olefins, the products are similar as are the spectral changes that accompany the reactions. They appear to occur by somewhat related mechanisms. In the product distribution for cyclohexene, both 2-electron (alcohol) and 4-electron (ketone) products appear whose relative amounts vary with the $Ru^{IV}{=}O^{2+}$ to olefin ratio. The ketone dominates when this ratio is high with the alcohol increasing from <10% at 2:1 to ~50% at 1:50. In the oxidation of indene, the allylic ketone is the only product even at $Ru^{IV}{=}O^{2+}$:indene ratios as high as 1:50.

The results of the various kinetics and product studies allow detailed mechanisms to be proposed for these reactions. They are complex, multistep processes similar in complexity to the epoxidation of olefins by $Ru^{IV}{=}O^{2+}$ reported earlier.[12] There are three discernible stages in both reactions: (1) reduction of Ru(IV) to Ru(III), (2) reduction of Ru(III) to Ru(II), and (3) solvolysis of Ru(II). The degree to which they overlap kinetically depends on the olefin concentration with the three stages well separated at high olefin concentrations.

Oxidation of Cyclohexene. The Ru(IV) → Ru(III) Stage. The results of a number of experiments provide direct evidence about the details of the first stage of cyclohexene oxidation in which Ru(IV) is reduced to Ru(III). (1) The reaction is first-order in both $Ru^{IV}{=}O^{2+}$ and olefin. The spectral changes are consistent with reduction of Ru(IV) to Ru(III) (predominantly as $Ru^{III}{-}OH^{2+}$). The same pattern of spectral changes is observed over a wide range of $Ru^{IV}{=}O^{2+}$ to olefin ratios with concentrations of cyclohexene as high as 1 M. (2) Addition of hydroquinone after the first stage causes rapid reduction of Ru(III) to Ru(II). Two products form, $Ru^{II}{-}OH_2^{2+}$ and a Ru(II) intermediate ($\lambda_{max} \approx 442$ nm), Ru(II)′. The latter undergoes solvolysis with $k_{solv} = (1.28 \pm 0.04) \times 10^{-2}\ s^{-1}$. The ratio of $Ru^{II}{-}OH_2^{2+}$ to Ru(II)′ is 4−5:1. (3) At $Ru^{IV}{=}O^{2+}$:cyclohexene = 2:1, the product is principally 2-cyclohexen-1-one (92%, Table 2). Oxidation of 3,3,6,6-tetradeuterocyclohexene under these conditions gives largely unrearranged ketone (Table 3) which is consistent with a mechanism in which cyclohexenyl radical is not formed. (4) From the rate constant data for the α,α′-H_4 and α,α′-D_4 olefins, there is a H/D kinetic isotope effect of 21 ± 1 for the reaction between $Ru^{IV}{=}O^{2+}$ and cyclohexene. (5) From the ^{18}O-labeling results, the O-atom in the ketone product comes from the oxo group of $Ru^{IV}{=}O^{2+}$ and not from H_2O in the solvent. (6) The organic product of the Ru(IV) → Ru(III) stage remains bound to Ru(III) and is the ketone as shown by FTIR. It is released following hydroquinone reduction of Ru(III) to Ru(II) as shown by GC−MS analysis. 2-Cyclohexen-1-ol only appears as a product at the Ru(III) → Ru(II) stage (see below).

On the basis of these results, the first step appears to be insertion of $Ru^{IV}{=}O^{2+}$ into an α-C−H bond by a nonradical pathway with O-atom transfer. This would give a bound alcohol,

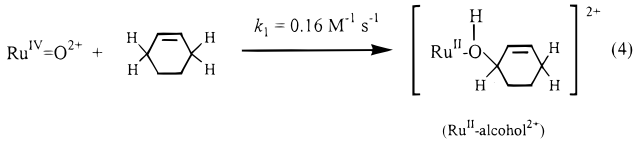

(4)

but the initial product formed is the ketone bound to Ru(III) rather than the alcohol bound to Ru(II). To explain these observations, it is necessary to invoke rapid oxidation of the initial Ru^{II}-alcohol^{2+} intermediate by $Ru^{IV}{=}O^{2+}$.

There is an additional complication in that the expected ν(C=O) stretch for a ketone bound to Ru(III) does not appear in the FTIR spectrum. Given this observation, the Ru(III) intermediate is probably better formulated as the enol

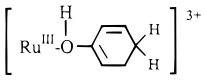

or enolate,

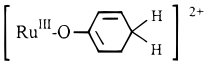

The bound alcohol should be acidic. The pK_a for loss of a proton from *cis*-$[Ru^{III}(bpy)_2(py)(H_2O)]^{3+}$ is 0.85.[15]

Assuming the enolate, further oxidation of the Ru^{II}-alcohol^{2+} intermediate occurs by

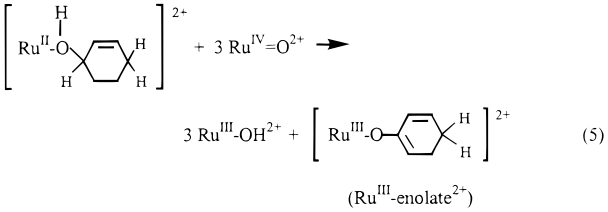

(5)

The net reaction is

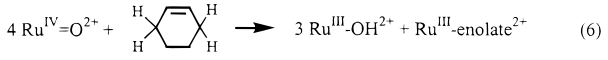

(6)

This reaction is consistent with the evidence for two different forms of Ru(III) at the end of the Ru(IV) → Ru(III) stage.

Ru(III) → Ru(II) Stage. In the second stage, Ru(III) is reduced to Ru(II), and the free ketone appears as a product in solution. The alcohol also begins to appear as a product at this stage. Absorbance-time traces can be simulated by a mechanism in which there is initial disproportionation, eq 3, followed by $Ru^{IV}{=}O^{2+}$ oxidation of cyclohexene, eqs 4 and 5.

To explain the data in Tables 2 and 3, it is necessary to invoke a competing parallel pathway. At $Ru^{IV}{=}O^{2+}$:olefin = 2:1, the product is largely ketone with nearly complete ^{18}O transfer and no allylic rearrangement. As this ratio is increased, the alcohol

product appears. There is incomplete ^{18}O transfer, and some allylic rearrangement occurs. The yield of alcohol increases from 8% at $Ru^{IV}{=}O^{2+}$:olefin = 2:1 to 53% at 1:50.

Given these observations, the parallel pathway may occur by 1-electron oxidation by $Ru^{III}{-}OH^{2+}$ to give the cyclohexyl radical

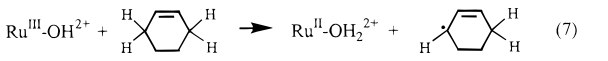

(7)

From known autoxidation chemistry, this would be followed by O_2 oxidation in a radical chain mechanism,[9,10] possibly with

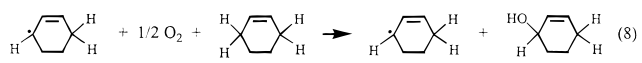

(8)

termination by

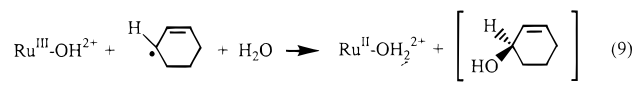

(9)

Given the ^{18}O-labeling results in Table 3, the O-atom in the alcohol product is not derived from the oxo group of $Ru^{IV}{=}O^{2+}$ or from H_2O and must come from O_2.

Once formed under close to stoichiometric conditions, the alcohol is more reactive toward oxidation by $Ru^{IV}{=}O^{2+}$ than the olefin by a factor of 14 ($k = 1.10$ versus 0.16 M^{-1} s^{-1}) and would not build up in the solution.

A radical pathway at higher olefin to $Ru^{IV}{=}O^{2+}$ ratios would explain both the appearance of allylic rearrangement and the less than complete ^{18}O transfer in the ketone product. The alcohol is favored as the olefin concentration is increased because direct oxidation by $Ru^{III}{-}OH^{2+}$ (eq 7) becomes increasingly competitive with disproportionation and oxidation by $Ru^{IV}{=}O^{2+}$. Direct oxidation increases in importance as the reaction proceeds, and [$Ru^{III}{-}OH^{2+}$] decreases since the rate of disproportionation depends on the square of the $Ru^{III}{-}OH^{2+}$ concentration.

The oxidative equivalent in the putative Ru^{III}-enolate^{2+} intermediate may contribute both to disproportionation and direct oxidation:

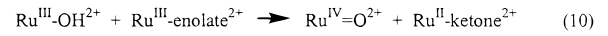

(10)

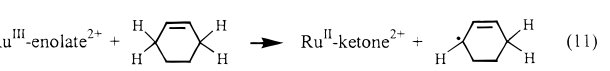

(11)

A product of both is Ru^{II}-ketone^{2+} which, from the quenching experiments with added hydroquinone, undergoes solvolysis with $k = (1.28 \pm 0.04) \times 10^{-2}$ s^{-1}.

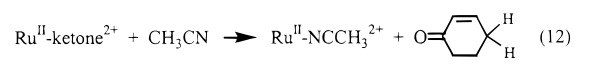

(12)

This reaction and the solvolysis of $Ru^{II}{-}OH_2^{2+}$ comprise the slow, third stage of the reaction.

Oxidation of Indene. Ru(IV) → Ru(III) Stage. The oxidation of indene by $Ru^{IV}{=}O^{2+}$ is also first-order in olefin and $Ru^{IV}{=}O^{2+}$ but is more rapid than cyclohexene by a factor of 36. $Ru^{III}{-}OH^{2+}$ is a product along with a second component having $\lambda_{max} \approx 550$ nm. There is no FTIR evidence for ν(C=O) of a coordinated ketone complex although the only product at the end of the reaction is indenone. With $Ru^{IV}{=}{}^{18}O^{2+}$ as the oxidant and $Ru^{IV}{=}O^{2+}$:indene = 1:1, the indenone product is ~80% ^{18}O-labeled with little incorporation from added $H_2{}^{18}O$. Addition of excess hydroquinone or ascorbic acid at the end of this stage gives $Ru^{II}{-}OH_2^{2+}$ and a second component which solvolyzes to give $Ru^{II}{-}NCCH_3^{2+}$ with $k_{solv} = (2.6 \pm 0.2) \times 10^{-2}$ s^{-1}. The ratio of $Ru^{II}{-}OH_2^{2+}$ to intermediate is ~1.4:1.

Oxidation of indene also appears to occur by insertion

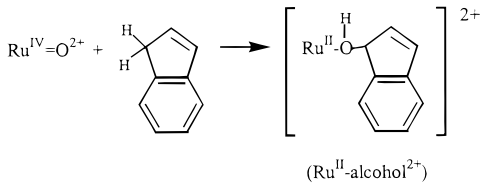

(13)

followed by further oxidation to an Ru^{III}-alkoxide^{2+} intermediate

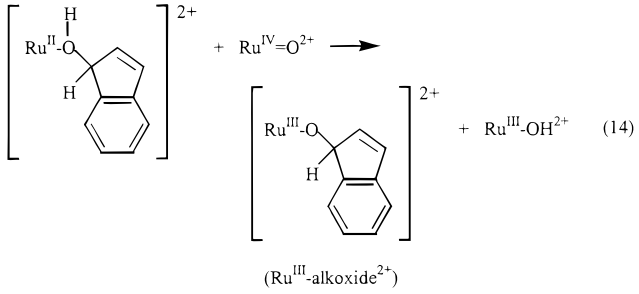

(14)

The net reaction is

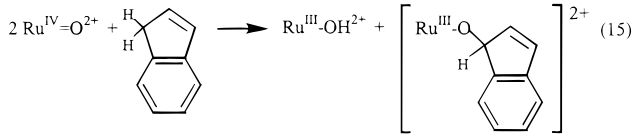

(15)

With this interpretation, the low-energy absorption feature at ~550 nm could be an alkoxide → Ru(III) charge-transfer band in Ru^{III}-alkoxide^{2+} which, upon reduction, gives Ru^{II}-alcohol^{2+} as the observed intermediate. An analogous N_{3-} → Ru(III) band appears at 498 nm ($\epsilon = 7370$ M^{-1} cm^{-1}) for [$Ru^{III}(bpy)_2(py)(N_3)$]$^{2+}$ in CH_3CN.[21]

The principal difference in behavior between the oxidations of cyclohexene and indene at this stage is in the extent of oxidation with indene oxidized by two electrons and cyclohexene by four. The difference can be rationalized if the key to 4-electron oxidation is proton loss and formation of a bound enolate. A Ru^{III}-enolate^{2+} form is inaccessible for indene because there is no dissociable C−H proton.

The mechanism in eqs 14 and 15 predicts a $Ru^{II}{-}OH_2^{2+}$:Ru^{II}-alcohol^{2+} ratio of 1:1 following hydroquinone or ascorbic acid reduction of Ru(III). The experimental value is ~1.4:1. Also, when $Ru^{IV}{=}{}^{18}O^{2+}$ is the oxidant, only ~80% of the indenone is ^{18}O-labeled, and the O-atom in the unlabeled portion does not come from H_2O (Table 3).

These two observations suggest that a competing reaction may exist at the Ru(IV) → Ru(III) stage, perhaps 1-electron transfer to give the indenyl radical,

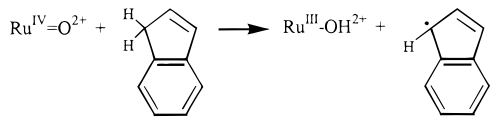

(16)

(21) Brown, G. M.; Callahan, R. W.; Meyer, T. J. *Inorg. Chem.* **1975**, *14*, 1915.

Scheme 3

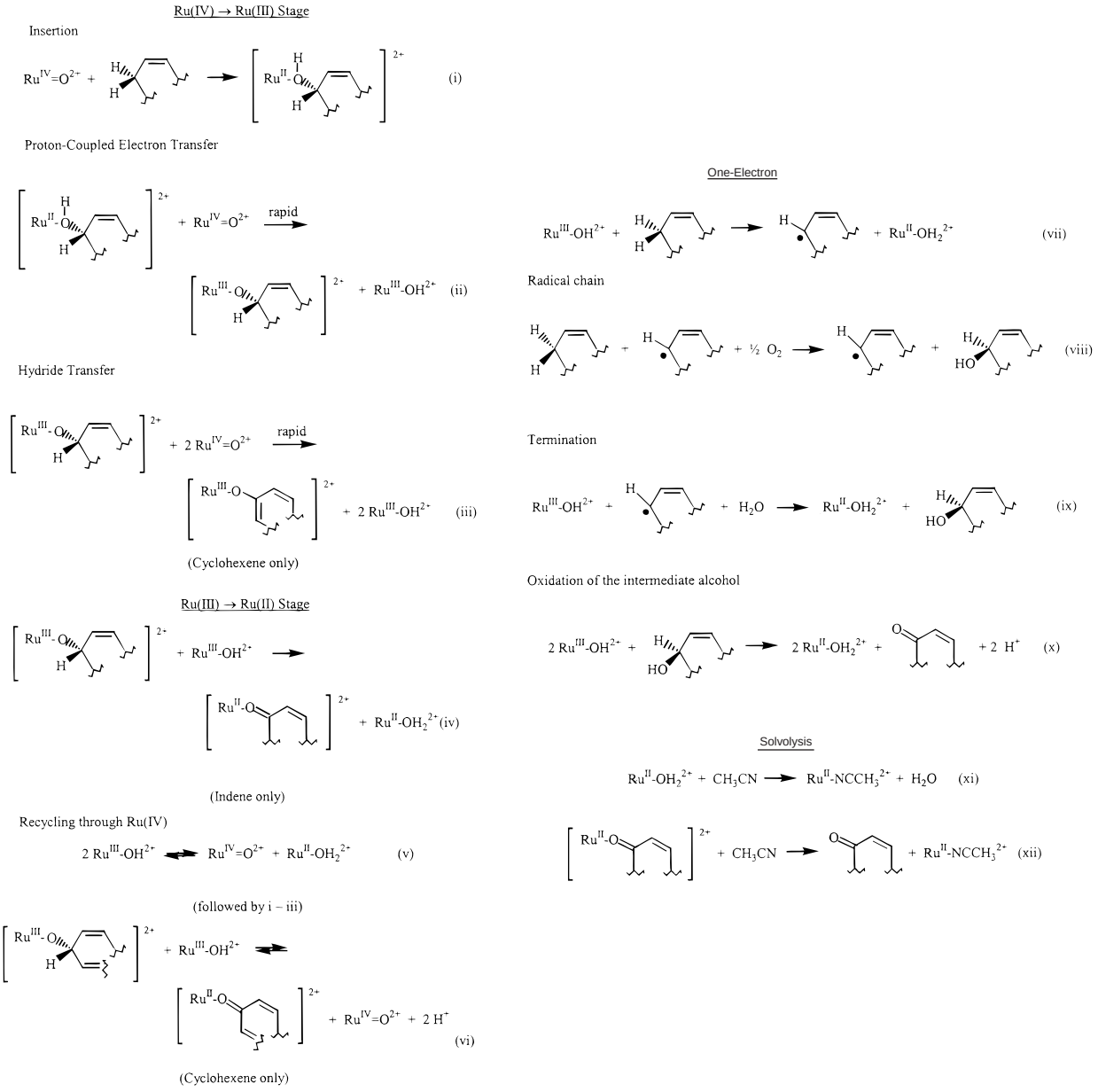

Radical chain autoxidation would give the alcohol,

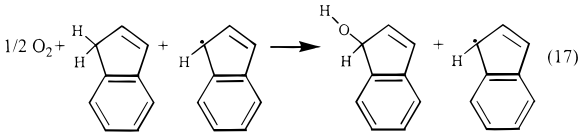

and further oxidation by $Ru^{IV}{=}O^{2+}$, indenone.

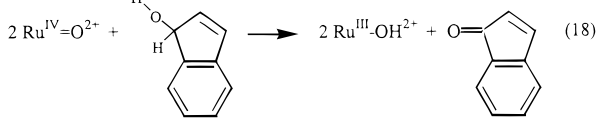

Ru(III) → Ru(II) Stage. In the reduction of Ru(III) to Ru(II), $Ru^{III}{-}OH^{2+}$ and Ru^{III}-alkoxide^{2+} are simultaneously reduced to Ru(II) to give $Ru^{II}{-}OH_2^{2+}$ ($k_{solvolysis} = k_4 = 1.66 \times 10^{-3}\ s^{-1}$) and Ru^{II}-ketone^{2+}. The ketone intermediate undergoes solvolysis with $k = 1.2 \times 10^{-2}\ s^{-1}$ to give free ketone, ν(C═O) at 1712 cm^{-1}. The same rate constant for solvolysis was obtained by FTIR and UV−visible monitoring. In a related reaction, Keene et al.[22] investigated the intramolecular oxidation of a chelated alkoxide to the aldehyde. The kinetics were consistent with initial disproportionation to Ru(II) and Ru(IV) followed by rate-limiting proton release and internal oxidation.

This is not the case here where there is a first-order dependence on Ru(III), and yet $Ru^{II}{-}OH_2^{2+}$ and Ru^{II}-ketone^{2+} appear simultaneously. This suggests a mechanism in which a reactive form of the alkoxide complex undergoes oxidation by $Ru^{III}{-}OH^{2+}$ as in eq 19.

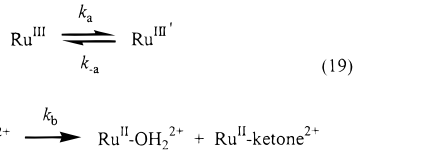

(22) Ridd, M. J.; Gakowski, D. J.; Sneddon, G. E.; Keene, F. R. *J. Chem. Soc., Dalton Trans.* **1992**, 1949.

Table 5. Summary of Oxidations Involving *cis*-$[Ru^{IV}(bpy)_2(py)(O)]^{2+}$ in CH_3CN or H_2O

reductant	solvent	product	k (25 °C M^{-1} s^{-1})	k_H/k_D	$\Delta H^{\ddagger}$ (kcal mol^{-1})	$\Delta S^{\ddagger}$ (cal deg^{-1} mol^{-1})	ref
cyclohexene	CH_3CN	2-cyclohexen-1-one	0.16 ± 0.01	21 ± 1	7.4 ± 0.1[b]	-34 ± 3.4[b]	this work
indene	CH_3CN	indenone	5.74 ± 0.74				this work
trans-stilbene	CH_3CN	trans-stilbene oxide	0.278 ± 0.002		4.4 ± 0.1	-46 ± 0.4	12
hydroquinone	H_2O	benzoquinone	$(9.6 \pm 0.3) \times 10^5$	28.7 ± 1.0	0.64 ± 0.04	-29.0 ± 0.1	20
H_2O_2	H_2O	O_2	1.74 ± 0.18	22.0 ± 1.2	6.0 ± 0.3	-37 ± 3	29
phenol	CH_3CN	benzoquinone	$(1.9 \pm 0.4) \times 10^2$	5.5 ± 0.2	10.3 ± 0.6	-14 ± 2	13
PPh_3	CH_3CN	$OPPh_3$	1.60 ± 0.02[a]		4.7 ± 0.5	-19 ± 3	26
$S(CH_3)_2$	CH_3CN	$OS(CH_3)_2$	1.71×10^1		8.0 ± 0.8	-26 ± 3	25
$OS(CH_3)_2$	CH_3CN	$O_2S(CH_3)_2$	1.34×10^{-1}		6.8 ± 0.2	-39 ± 3	25
$PhCH_2OH$	H_2O	PhCHO	2.43 ± 0.03	50 ± 3	5.8 ± 0.4	-38 ± 1	21
$[Ru^{II}(bpy)_2(py)(OH_2)]^{2+}$	CH_3CN	$[Ru^{III}(bpy)_2(py)(OH)]^{2+}$	$(4.07 \pm 0.13) \times 10^3$	14.6 ± 0.7			27

[a] Measured at 25.8 ± 0.2 °C. [b] See ref 28.

According to this mechanism, $k_{obs} = k_a$ in the limit, $k_b \gg k_{-a}$ with $k_{obs} = k_a$. In this limit, the rate determining step is conversion of Ru^{III}-alkoxide^{2+} to the activated form. One possibility for the activated form is proton migration,

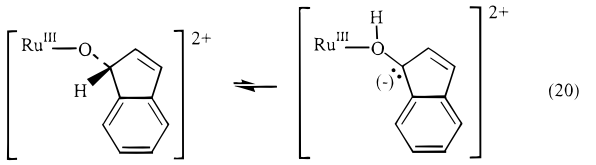

(20)

to give a carbanion intermediate stabilized by electronic delocalization to Ru(III).

Mechanistic Summary. A global summary of the mechanisms for oxidation of cyclohexene and indene is given in Scheme 3.

Most allylic oxidations by transition metal complexes occur by radical autoxidation mechanisms. $Ru^{IV}{=}O^{2+}$ is capable of allylic oxidation but without the intervention of radical pathways. The radical chemistry, that does occur, has its origin in $Ru^{III}{-}OH^{2+}$ and not in $Ru^{IV}{=}O^{2+}$.

There are important implications for synthesis in the mechanism in Scheme 3. The initial reaction appears to be a concerted process that gives an alcohol product. Further oxidation gives the ketone and Ru(III) intermediates. They complicate the mixture of products by initiating 1-electron, radical chemistry. A related complication has been observed from Ru(III) in the epoxidations of *cis*- and *trans*-stilbene and styrene by *cis*-$[Ru(bpy)_2(py)(O)]^{2+}$.

These results point to an advantage in immobilizing the oxidant on a surface or in a membrane as a way of limting oxidation to the alcohol stage. We are currently investigating this possibility on high surface area oxide supports.

Mechanism of Oxidative Insertion. Oxidative insertion into an allylic C−H bond occurs in the first step in Scheme 3. An argument could be made for consecutive 1-electron steps and a Ru(III) alkoxy radical intermediate with a lifetime too short for allylic rearrangement to occur. However, it should be noted that there is a significant kinetic advantage for $Ru^{IV}{=}O^{2+}$ compared to $Ru^{III}{-}OH^{2+}$ even though they have comparable redox potentials. With reductants that undergo 1-electron transfer by proton-coupled electron-transfer such as hydroquinone,[20] rate constants are comparable. Compared to $Ru^{IV}{=}O^{2+}$, oxidation of olefins by $Ru^{III}{-}OH^{2+}$ occurs by 1-electron transfer and far more slowly.

Given the magnitude of the kinetic isotope effect for cyclohexene, oxidative insertion probably occurs through an asymmetrical transition state at which there is extensive C−H bond breaking. In this reaction, the electron flow is from the σ(C−H) molecular orbital

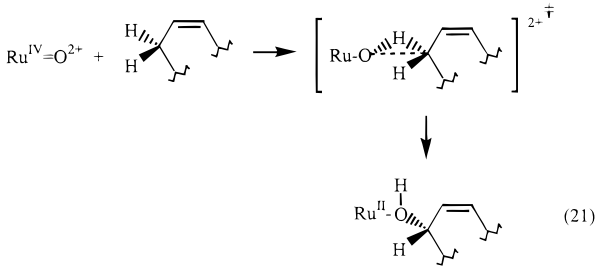

(21)

to the lowest acceptor orbital or orbitals at $Ru^{IV}{=}O^{2+}$. These are a pair of orbitals, $d\pi^*_{Ru}$, largely $d\pi$ in character but antibonding with regard to the Ru−O interaction through mixing with oxygen 2p orbitals. There is a double vacancy in this set of orbitals which allows $Ru^{IV}{=}O^{2+}$ to function as a 2-electron acceptor.

This mechanism can be added to others whose details have been elucidated in earlier studies and are summarized in Table 5. They include hydride transfer from alcohols,[23] electrophilic oxo attack on phenol with net C−H insertion,[24] oxygen atom transfer to sulfides[25] and phosphines,[26] oxygen atom transfer in the epoxidation of olefins,[12] and proton-coupled electron transfer in the oxidations of hydroquinones[20] and $Ru^{II}{-}OH_2^{2+}$.[27]

Acknowledgment is made to the National Science Foundation under Grant No. CHE-9503738 and to the Department of Energy under Grant No. LM 19X-SX 092C for support of this research.

Supporting Information Available: Procedure of generating calibration curves for analysis, procedure of product analysis, and Figures S1−9 (PDF). This material is available free of charge via the Internet at http://pubs.acs.org.

JA991722X

(23) Thompson, M. S.; Meyer, T. J. *J. Am. Chem. Soc.* **1982**, *104*, 4106. (b) Roecker, L. E.; Meyer, T. J. *J. Am. Chem. Soc.* **1987**, *109*, 746.
(24) Seok, W. K.; Meyer, T. J. *J. Am. Chem. Soc.* **1988**, *110*, 7358. (b) Seok, W. K.; Dobson, J. C.; Meyer, T. J. *Inorg. Chem.* **1988**, *27*, 3.
(25) Roecker, L. E.; Dobson, J. C.; Vining, W. J.; Meyer, T. J. *Inorg. Chem.* **1987**, *26*, 779.
(26) Moyer, B. A.; Sipe, B. K.; Meyer, T. J. *Inorg. Chem.* **1981**, *20*, 1475.
(27) Binstead, R. A.; Moyer, B. A.; Samuels, G. J.; Meyer, T. J. *J. Am. Chem. Soc.* **1981**, *103*, 2897.
(28) Curry, M. E. Ph.D. Dissertation, University of North Carolina at Chapel Hill, NC, 1990.
(29) Gilbert, J. A.; Gersten, S. W.; Meyer, T. J. *J. Am. Chem. Soc.* **1982**, *104*, 6872.